II CONGRESSO NACIONAL DE ENGENHARIA MECÂNICA
II NATIONAL CONGRESS OF MECHANICAL ENGINEERING
12 a 16 de Agosto de 2002 - João Pessoa – PB

DISPLACEMENT OF NEWTONIAN AND NON NEWTONIAN LIQUIDS IN A CAPILLARY TUBE

Edson J. Soares (edsonjs@mec.puc-rio.br)

Paulo Roberto de Souza Mendes (pmendes@mec.puc-rio.br)

Márcio da S. Carvalho (msc@mec.puc-rio.br)

Department of Mechanical Engineering
Pontifícia Universidade Católica do Rio de Janeiro (PUC-Rio)
Rua Marquês de São Vicente 225, Gávea
22453-900, Rio de Janeiro, RJ, Brazil

Abstract. *The displacement of a fluid in a capillary tube by gas injection occurs in many practical applications like enhanced oil recovery, coating of catalytic converters and gas-assisted injection molding. This situation has been extensively studied both by theory and experiments in the case of Newtonian fluids, however the complete understanding of the effects of the rheological properties of the displaced fluid in this type of flow is still under investigation. Recent work has shown that, at a given Capillary number, the amount of shear thinning liquid deposited on the tube wall falls with decreasing power-law exponent, but a singular perturbation method was not able to capture this effect. The flow of viscoelastic liquids has also been analyzed experimentally by measuring the fractional coverage of the tube walls and by Particle Tracking Velocimetry. The main conclusion was that the flow near the interface presents strong extensional deformation and that the viscoelastic behavior of the liquid leads to larger deposited liquid layer on the wall. Flow simulation with non Newtonian liquids for this situation is rare. The presence of the free surface and the non linearities of the constitutive model make the problem extremely complex. In this work, the complete two dimensional solution of the free surface flow is obtained using the Galerkin finite element method. The rheological character of the liquid is modeled by two different constitutive equations: a simple Generalized Newtonian Liquid model, to analyze the effect of shear sensitive liquids; and the algebraic constitutive relation proposed by Thompson et al. (1999) that is capable of describing variable shear and extensional viscosity, first normal stress coefficient and second normal stress coefficient. This constitutive equation is used to analyze the effect of the viscoelastic properties of the liquid on the flow field.*

Keywords: *Gas displacement, non Newtonian liquids, finite element method, free surface flows.*

1. INTRODUCTION

The gas displacement of a fluid in a capillary tube occurs in many practical applications like enhanced oil recovery, coating of catalytic converters and gas-assisted injection molding. As the gas pushes the liquid through the tube, a thin liquid layer is left attached to the wall. The thickness of this liquid film is an important parameter in many of the applications mentioned before: in the case of oil recovery, the amount of liquid left on the wall determines the efficiency of the recovery process; and in the case of gas-assisted injection molding, the thickness of the layer will determine the strength of the hollow part produced.

The flow of a gas penetrating a Newtonian liquid has been extensively studied both by theory and experiments. The goal was to understand the flow near the gas-liquid interface in order to determine the amount of liquid left on the tube wall as a function of the operating parameters and liquid properties.

However, in many of the practical applications, the liquid being displaced is a polymer melt, solution or a dispersion that show non Newtonian behavior. The complete understanding of the effects of the rheological properties of the displaced liquid in this type of flow is still under investigation.

The thickness of the thin liquid layer attached to the wall is usually characterized in terms of the fractional deposited mass m, defined as

$$m = \frac{R_0^2 - R_b^2}{R_0^2} = \frac{V_b - \overline{U}}{V_b}.$$

R_0 is the tube radius and R_b is the radius of the gas bubble, as illustrated in Fig.(1). The fractional mass can also be evaluated as a function of the bubble velocity V_b and the mean velocity $\overline{U}$ of the liquid ahead of it.

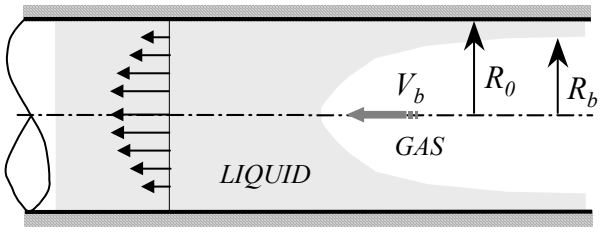

Figure 1. Sketch of gas displacement of a liquid in a capillary tube.

The first experimental analysis of gas-assisted displacement was done by Fairbrother and Stubs (1935). They found an expression for m valid at small capillary numbers $Ca \equiv \mu V_b / \sigma$ and Newtonian liquid:

$$m = Ca^{1/2}$$

Taylor (1960) studied the same problem for a much larger range of capillary number. He found that the mass deposited on the tube wall asymptotically approaches 0.55 as *Ca* approaches 2. Taylor also suggested three possible streamline patterns of the liquid flow near the interface. At high capillary number, the flow would pass completely and no recirculation would appear near the free surface. The other two patterns would occur at intermediate to low capillary numbers, and they would be characterized by the position of the recirculation near the free surface.

Cox (1962), continuing Taylor's study for a Newtonian viscous fluid, found experimentally that the amount of mass deposited on the tube wall asymptotically reaches 0.60 as the capillary number approaches 10. Cox also predicted the shape of the interface using perturbation analysis. He concluded that the flow is sensitive to the presence of the interface only in a region about one and a half the tube diameter ahead the nose of the bubble. Furthermore, he concluded that the bubble reaches its final shape after it flows the same distance (one and a half the tube diameter). In a second work, Cox (1964) investigated experimentally the streamline patterns suggested by Taylor and found a good agreement in the cases of high and low capillary number.

Bretherton (1960) investigated theoretically and experimentally the motion of long gas bubbles in tubes filled with Newtonian viscous liquid. He found a simple theoretical relationship for the

mass deposited on the tube wall m, valid at low capillary number, that agrees well with Fairbrother and Stubs (1935) experimental measurements:

$$m = 1.29\left(3\frac{\mu V_b}{\sigma}\right)^{2/3}$$

The penetration of long gas bubble in a viscoelastic liquid was studied experimentally by Huzyak and Koelling (1997). They were interested in identifying the influence of viscoelastic behavior on the fraction of the mass deposited on the tube wall. The experiments were performed with highly elastic liquid with constant shear viscosity. The results were presented in terms of capillary number Ca and Deborah number De. They found that the fractional mass deposited on the wall begins to increase, relatively to Newtonian fluid, for $De \geq 1$ and continues increasing over the entire range of De analyzed. Following the work of Huzyak and Koelling, Gauri and Koelling (1999) analyzed the kinematics of the flow near the free surface using Particle Tracking Velocimetry (PTV).

The effect of shear thinning behavior of the displaced liquid in this type of flow was studied by Poslinski and Coyle (1994). They used the Finite Element Method to solve the two dimensional model of the flow. Kamisli and Rayan (1999) performed experiments and showed that the thickness of the deposited layer falls with the power-law index. They presented a singular perturbation analysis to model this situation, but their predictions followed an opposite trend of the experimental results.

Theoretical analysis of the effect of different rheological properties other than the shear dependent viscosity is rare. The presence of the free surface and the non-linearities of the constitutive models make the problem extremely complex.

One possible approach to model gas penetration through a viscoelastic liquid is to use differential constitutive equations, such as Giesekus model. However, the solution of the momentum equation coupled with this type of constitutive equations is a major numerical challenge and solutions cannot be obtained at the range of dimensionless parameters that occurs in practical applications. An alternative way is to use algebraic models that relate stress to the rate-of-strain and relative-rate-of-rotation. These models are perhaps the simplest and computationally most economical attempt at capturing the different behavior of polymer molecules in extension-dominated and shear-dominated flow zones. Recent advances in this class of models have produced a constitutive relation that describes shear thinning and normal stress differences in simple shear flow and extensional thickening in extensional flows. This tatic is pursued here.

In this work, the complete two dimensional solution of the free surface flow is obtained using the Galerkin finite element method. The rheological character of the liquid is modeled by two different constitutive equations: a simple Generalized Newtonian Liquid model, to analyze the effect of shear sensitive liquids; and the algebraic constitutive relation proposed by Thompson et al (1999). This equation is used to analyze the effect of the viscoelastic properties of the liquid on the flow field. The theoretical predictions are compared with some of the experimental data for non Newtonian liquids available in the literature.

2. STEADY LIQUID DISPLACEMENT MODEL

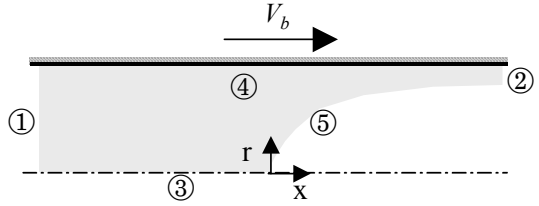

Figure 2. Flow domain for gas displacement of liquids in a tube.

When a gas is injected at a constant rate in a capillary tube displacing a liquid, a thin layer of liquid is left on the wall of the tube. The thickness of this layer is important in many of the processes described in the previous section and is a strong function of the operating conditions and liquid properties.

The flow near the gas-liquid interface is analyzed using a moving reference frame placed at the tip of the bubble, as shown in Fig.(2). In the figure, the interface is moving from right to left. Relative to the reference frame, the capillary tube wall moves with the interface velocity V_b and the interface is stationary.

2.2. Conservation Equations and Boundary Conditions

The flow near the interface is two-dimensional and axisymmetric. The velocity and pressure fields, and the configuration of the gas-liquid interface are governed by the momentum and continuity equations:

$$\rho \mathbf{v} \cdot \nabla \mathbf{v} - \nabla \cdot \mathbf{T} = 0 \quad \text{and} \quad \nabla \cdot \mathbf{v} = 0 \tag{1}$$

together with the appropriate boundary conditions. **v** is the velocity field and **T** is the stress tensor. Ω represents the physical domain where the differential equations are posed.

Far enough upstream of the interface, boundary (1), the flow is taken to be fully developed and the pressure constant. Far enough downstream, boundary (2), the liquid traction vanishes. Along the symmetry axis (3), the shear stress and the radial velocity vanish. The no-slip, no-penetration conditions is applied along the tube wall (4). Over the gas-liquid interface (5), the traction in the liquid balances the capillary pressure and there is no mass flow across the interface:

$$\mathbf{n} \cdot \mathbf{T} = \sigma \frac{d\mathbf{t}}{ds} - P_0 \mathbf{n} \quad \text{and} \quad \mathbf{n} \cdot \mathbf{v} = 0 . \tag{2}$$

σ is the liquid surface tension, ***t*** is the unit vector tangent to the free surface and *s* is an arc-length coordinate along the interface and $d\mathbf{t}/ds$ is the local curvature of the interface.

2.3. Constitutive Models

In order to close the set of differential equations, the stress tensor has to be related with the kinematics of the flow. Here, two different non Newtonian models are used. The first is a simple Generalized Newtonian Model with a Power-Law viscosity function. The second is the algebraic model proposed by Thompson et al. (1999) that takes into account the different behavior of polymer molecules in extension-dominated and shear-dominated flow zones.

2.3.1. Generalized Newtonian Model: Power-law viscosity

In this simple model, the stress tensor is given by

$$\mathbf{T} = -p\mathbf{I} + \eta(2\mathbf{D})2\mathbf{D} , \tag{3}$$

where $2\mathbf{D} \equiv \nabla \mathbf{v} + \nabla \mathbf{v}^T$ is the rate of strain tensor. η is the liquid viscosity, that is a function of the deformation of the flow. In the particular case of a Power-Law viscosity function, it is given by

$$\eta = K \dot{\gamma}^{n-1} .$$

n is the power-law index and $\dot{\gamma}$ is the local deformation rate. In cylindrical coordinates, it is

$$\dot{\gamma} = \left[\left(\frac{\partial u}{\partial r} + \frac{\partial v}{\partial x} \right)^2 + 2\left(\frac{\partial u}{\partial x} \right)^2 + 2\left(\frac{\partial v}{\partial r} \right)^2 + 2\left(\frac{v}{r} \right)^2 \right]^{1/2}$$

2.3.2. Algebraic Viscoelastic Model

The algebraic model used here was proposed by Thompson et al. (1999). The stress tensor is a function of both the rate-of-strain tensor **2D** and the relative-rate-of-rotation tensor $\overline{\mathbf{W}}$:

$$\mathbf{T} = -p\mathbf{I} + \alpha_1 \mathbf{D} + \alpha_2 \overline{\mathbf{W}}^2 + \alpha_4 \left(\mathbf{D} \cdot \overline{\mathbf{W}} - \overline{\mathbf{W}} \cdot \mathbf{D} \right) \tag{4}$$

The relative-rate-of-rotation tensor is defined as $\overline{\mathbf{W}} = \mathbf{W} - \mathbf{\Omega}$, where $\mathbf{W} = \nabla \mathbf{v} - \nabla \mathbf{v}^{\mathrm{T}}$ is the vorticity tensor, and the tensor $\mathbf{\Omega}$ is the rate of rotation of the eigenvectors of the rate of strain. Based on the rate-of-strain and relative-rate-of-rotation tensors, Astarita (1979) defined the flow classification index R to measure the degree to which the fluid particle avoids stretching. It is defined as

$$R \equiv -\frac{tr(\overline{\mathbf{W}})}{tr(\mathbf{D})} \tag{5}$$

The index takes the value of 0 in pure extension and 1 in shear flows. Moreover, as the motion approaches a rigid body motion, i.e. as $\mathbf{D} \to 0$, it approaches infinity.

The coefficients $\alpha_i's$ depend on the material functions of the liquid:

$$\alpha_1 = 2\eta_s^R \eta_u^{1-R} \;\; ; \;\; \alpha_2 = -2f(R)\left[\psi_1 + 2\psi_2\right] \text{ and } \;\; \alpha_4 = g(R)\psi_1$$

The additional definitions needed before using eq.(4) are the forms of the functions $\eta_s, \eta_u, \psi_1,$ and ψ_2. One of the advantages of using such class of models is that the measurements of these material functions in shear and extensional flows can be independently fitted.

In the predictions presented in this work, the shear viscosity was constant, the extensional viscosity was a known function of the deformation rate and the normal stress effects were not considered, i.e.

$$\eta_s = \eta_0 \; ; \;\; \eta_u = \eta_0 \left\{ 1 + \left(\lambda_u \dot{\gamma} \right)^2 \right\}^{\frac{n_u - 1}{2}} \text{ ; and } \;\; \psi_1 = \psi_2 = 0$$

3. SOLUTION METHOD

Because of the free surfaces, the flow domain at each parameter is unknown a priori. In order to solve this free boundary problem by means of standard techniques for boundary value problems, the set of differential equations and boundary conditions posed in the unknown domain has to be transformed to an equivalent set defined in a known reference domain. This transformation is made by a mapping that connects the two domains, as shown in Fig.(3). A functional of weighted smoothness can be used successfully to construct the sorts of maps involved here. The inverse of the mapping that minimizes the functional is governed by a pair of elliptic differential equations identical with those encountered in diffusional transport with variable diffusion coefficients. The coordinates ξ and η of the reference domain satisfy

$$\nabla \cdot \left(D_\xi \nabla \xi \right) = 0 \quad \text{and} \quad \nabla \cdot \left(D_\eta \nabla \eta \right) = 0 \tag{5}$$

D_ξ and D_η are diffusion-like coefficients used to control element spacing. Boundary conditions are needed in order to solve the second-order partial differential equations (5). Along solid walls and synthetic inlet and outlet planes, the boundary is located by imposing a relation between the coordinates *x* and *r* from the equation that describes the shape of the boundary and stretching functions are used to distribute the points along the boundaries. The free boundaries (gas-liquid interfaces) are located by imposing the kinematic condition, eq.(2-b). The discrete version of the mapping equations is generally referred to as mesh generation equations.

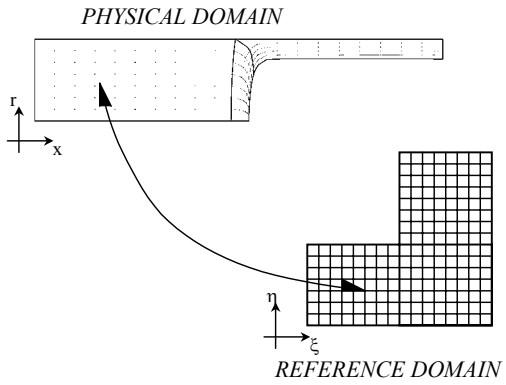

Figure 3. Mapping between physical and reference domain.

The Navier-Stokes system and the mapping (mesh generation) equations were solved all together by the Galerkin / finite element method. The velocity, pressure and node position are represented in terms of the appropriate basis functions: biquadratic for velocity and node position and piecewise linear discontinuous for pressure. Because the stress tensor depends on the second derivative of the velocity field (through the definition of the index *R*), an additional variable **L** is introduced to represent the velocity gradient with a continuous interpolation. It is also represented in terms of bilinear basis functions.

Once all the variables are represented in terms of the basis functions, the system of partial differential equations reduces to simultaneous algebraic equations for the coefficients of the basis functions of all the fields. This set of equations is non-linear and sparse. It was solved by Newton's method, and quadratic convergence was obtained as the residual approached zero. The linear system of equations at each Newton iteration was solved using a frontal solver.

The domain was divided into 240 elements with 4860 unknowns. A representative mesh is shown in Fig.(4).

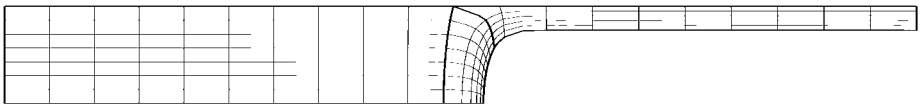

Figure 4. Representative Finite Element Mesh: 240 elements and 4860 unknowns.

4. RESULTS

The relevant dimensionless parameters for this problem are the Reynolds number $\mathrm{Re} = \rho V_b R_0 / \eta$, the capillary number $Ca = \eta V_b / \sigma$, the power law index *n* in the case of the Generalized Newtonian Model with a Power-Law viscosity function; and the Deborah number $De = \lambda_e V_b / R_0$, when the algebraic model is used. The results presented here were obtained at

negligible inertial forces, i.e. $Re = 0$. The main goal was to study the effect of the capillary number and rheological properties of the liquid on the flow near the liquid / gas interface.

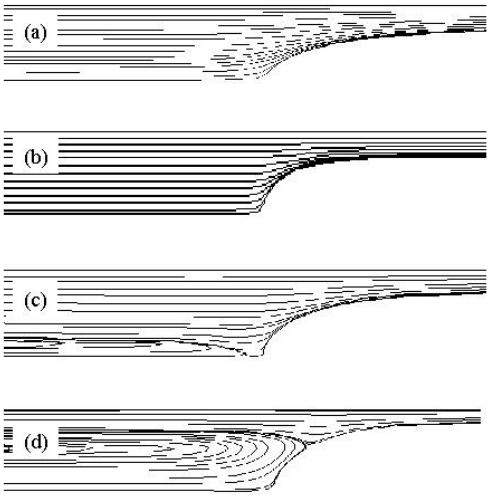

Figure 5. Streamline pattern near the free surface:
(a)Ca = 10; (b) Ca = 1; (c) Ca = 0.6 and (d) Ca = 0.2.

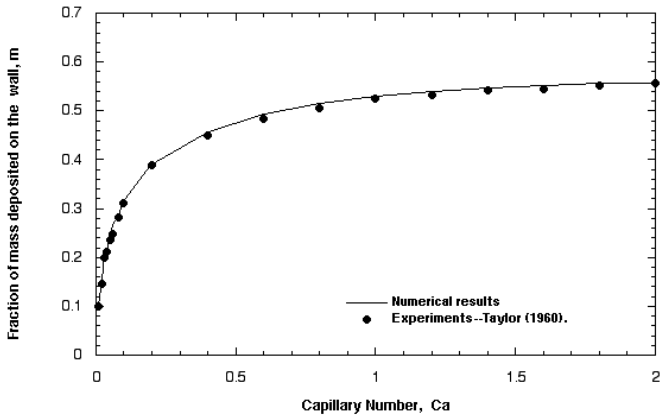

Figure 6. Fractional mass coverage as a function of capillary number for Newtonian Liquids.

The streamlines of a Newtonian flow at different capillary numbers are shown in Fig.(5). At high capillary number, the viscous force is stronger then the surface tension force and the adverse pressure gradient at the meniscus is small. There is no recirculation near the free surface and the film thickness left on the wall is relatively thick. As the capillary number falls, the film thickness on the wall decreases and a recirculation near the free surface appears. The three different patterns of streamlines suggested by Taylor (1961) do occur: One with no recirculation, at high capillary numbers; a second pattern with two stagnation points on the axis of the tube, obtained at moderate capillary numbers; and the third with a stagnation point at the tip of the bubble and a stagnation ring on the free surface.

The predictions of the Newtonian flow are in good agreement with experimental results. Figure (6) compares the fraction of mass deposited on the tube wall m predicted by the numerical simulation presented here with the measurements of Taylor (1960). The agreement is very good over the entire range of capillary number. The predicted interface configuration is also in good agreement with flow visualization reported by Cox (1966) and Huzyak and Koelling (1997), as illustrated in Fig.(7).

The effect of the Power Law index on the film thickness left on the wall is summarized in Fig.(8). It shows the predicted fractional mass coverage m as a function of capillary number obtained from gas penetration through a power-law liquid. The shear thinning behavior leads to

thinner film deposited on the wall over the entire range of capillary number. This trend agrees qualitatively with the experimental data presented by Kamisli and Rayan (1999), however the measured thickness of the liquid film left on the wall is lower than the theoretical predictions. The perturbation method presented by Kamisli and Rayan (1999) could not correctly predict the variation of the residual liquid film as a function of the Power-Law index. A complete two-dimensional model of the flow, as the one presented here is necessary to describe the non Newtonian flow near the free surface. One possible reason for the discrepancy between the theoretical results and the experiments is that viscosity dependence on shear rate of the two polymeric solutions used in the experiments, e.g. 1 % HEC and 1 % CMC, are not well described by a Power-Law function at the low deformation rate range. The Power-Law viscosity function can lead to unrealistic high viscosity at regions of the flow where the deformation rate is small.

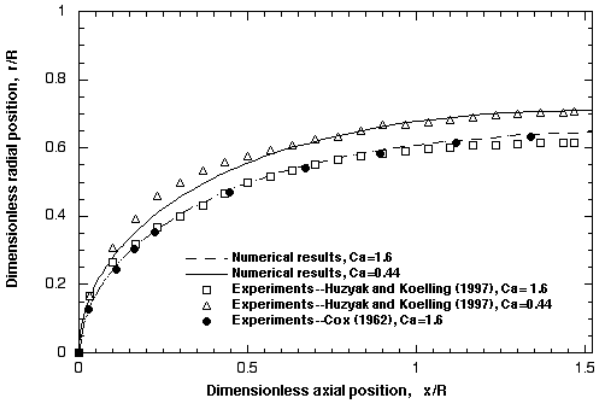

Figure 7. Comparison between predicted free surface profiles and experimental measurements.

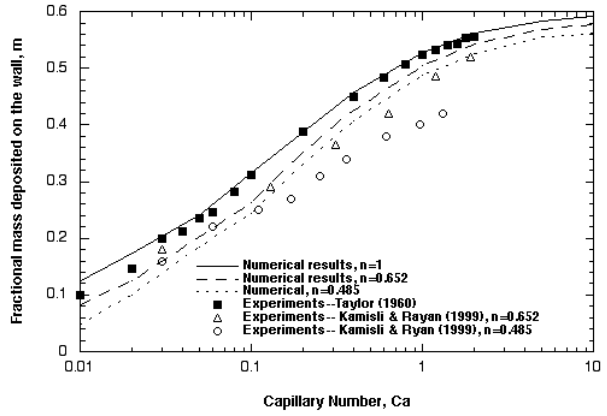

Figure 8. Fractional mass coverage as a function of capillary number for power-law liquids.

It is well known that the behavior of microstructured liquids in complex flows is very sensitive to the local kinematics. Polymer molecules behave quite differently in flow regions where the liquid is persistently stretched along the orientation of the molecules and in flow zones where the straining is oblique to molecular orientation. So, it is important to characterize the type of deformation suffered by liquid particles in different regions of the flow. The field of flow classification index R, defined in eq.(5), for the gas displacement flow is shown in Fig.(9). Far from the gas liquid interface $R \approx 1$ indicating a shear dominated flow, as expected. The liquid layer left on the tube moves as a rigid body. i.e. plug flow, and the value of R is high in that region. Near the free surface, $R \approx 0$ indicating an extensional dominated flow.

The ratio between the fractional mass deposited on the wall with a viscoelastic liquid to that of a Newtonian liquid as a function of the Deborah number, when the viscoelastic algebraic model is used, is shown if Fig.(10). The Capillary number was fixed at $Ca = 10$. The change in the amount of liquid left on the wall is very small and the film thickness falls with Deborah number. This prediction does not agree with the experimental measurements of deposited film thickness with

PEO solutions in water made by Huzyak and Koelling (1997). In their experiments, the fractional coverage *m* for the viscoelastic fluids begins to increase relative to the Newtonian results at $De \approx 1$, and it continues to rise with Deborah number for all $De > 1$. However the predictions confirm the experimental results of Bonn and Meunier (1997). They compared the flow configuration and the film thickness left on the wall when gas is displacing two different polymeric solutions: PEO in water and Xanthan gum in water. The shear viscosity of the two solutions tested was matched by controlling the molecular weight and concentration of each solution. Both liquids presented non Newtonian extensional viscosity, with Trouton ratio larger than 3, however only the PEO solution showed an increase in the film thickness deposited on the wall when compared to the Newtonian case. The deposited film thickness of Xantham gum solution was very close to the one obtained when a Newtonian liquid is used. The explanation was that the increase of the deposited thickness is related to the large first normal stress difference of the PEO solution. Because Xantham Gum is a rigid, rod-like polymer, the first normal stress coefficient is approximately zero. The theoretical predictions with the algebraic model were obtained with $\psi_1 = 0$ and therefore the model is more suitable to describe rigid rod-like polymer solutions, such as Xantham gum.

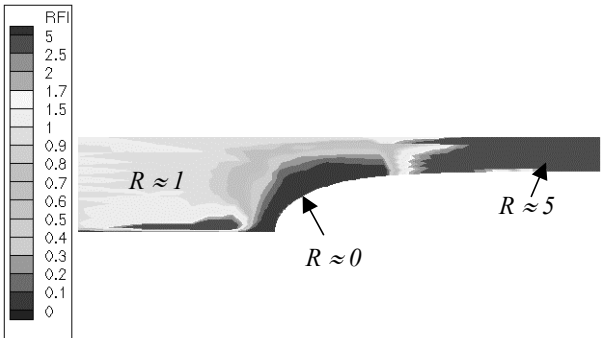

Figure 9. Flow classification index near the interface.

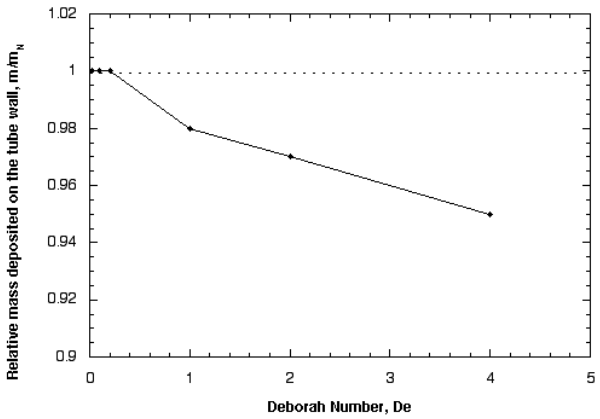

Figure 10. Fractional mass coverage as a function of Deborah number. Predictions obtained with the viscoelastic algebraic constitutive model.

5. FINAL REMARKS

A two-dimensional model of the flow near the gas-liquid interface of a long bubble penetrating through a liquid in a capillary tube was presented. The presence of the free surface makes the solution of the problem complex; the domain where the differential equations are integrated is unknown *a priori*. A fully coupled formulation was used and the differential equations were solved by the Galerkin Finite Element Method.

Two different constitutive models were used: a simple Generalized Newtonian Liquid model with a power-law viscosity function and an algebraic model that takes into account the different behavior of polymer molecules in extension-dominated and shear dominated flow zones.

The thickness of the liquid film on the tube wall and the interface profile for Newtonian liquids agree with experimental data available in the literature. The predictions with the power-law model followed the same trends observed experimentally, which could not be predicted with a perturbation analysis. The qualitative difference between the theoretical and experimental results may be caused by the unrealistic high viscosity yielded by the power-law model in regions of the flow where the deformation rate is small.

The theoretical predictions obtained with the algebraic non Newtonian model were limited to the case of vanishing normal stress differences. The only viscoelastic effect taken into account was the non Newtonian extensional viscosity with a Trouton ratio larger then 3. The liquid film thickness left on the wall was close to that of a Newtonian liquid, as observed in experiments with Xanthan Gum solutions, that also have a high Trouton ratio and vanishing normal stress difference.

The next step is to include normal stress data into the constitutive model. The theoretical predictions will be compared with data obtained with flexible polymer molecules, like PEO.

6. ACKNOWLEDGMENT

This research was partially funded by grants from the Brazilian Science and Technology Secretary MCT, the Brazilian Research Council CNPq and by the State of Rio de Janeiro Research Foundation FAPERJ.

7. REFERENCES

Astarita, G., 1979, J. Non-Newtonian Fluid Mechanics, vol. 6, pp.69-76.

Bretherton F. P., 1960, “The montion of long bubble in tubes”, J. Fluid Mechanics, vol.10, pp.166-188.

Cox, B. G., 1962, “On driving a viscous fluid out of a tube a tube”, J. Fluid Mechanics, pp.81-96.

Cox, B. G., 1964, “An experimental investigation of the streamlines in viscous fluid expelled from a tube”, J. Fluid Mechanics, vol.20, pp.193-200.

Fairbrother, F., Stubbs, A. E., 1935, J. Chem. Soc., vol.1, pp.527.

Gauri, V. , Koelling, K. W., 1999, “Gas-assisted displacement of viscoelatic fluids: flow dynamics at the bubble front”, J. Non-Newtonian Fluid Mechanics, vol.83, pp.183-203.

Huzyak, P. C., Koelling, K. W., 1997, “The penetration of a long bubble through a viscoelastic fluid in a tube”, J. Non-Newtonian Fluid Mechanics, vol. 71, pp.73-88.

Kamisli, F., Ryan, M. E., 1999, “Pertubation method in gas-assisted power-law fluid displacement in a circular tube and retangular channel”, Chemical Engineering Journal, vol.75, pp.167-176.

Poslinski A. J., Coyle, D. J., 1994, “Steady gas penetration through non Newtonian liquids in tube and slit geometries: isothermal shear thinning effects”, Proc. Polymer Processing Society, 10 Annual Meeting, pp.219.

Taylor, G. I., 1960, “Deposition of a viscous fluid on the wall a tube”, J. Fluid Mechanics, vol.10, pp.161-165.

Thompson, R. L., Souza Mendes, P. R., Naccache, M. F., 1999, “A new constitutive equation and its performance in contraction flows”, J.Non-Newtonian Fluid Mechanics, vol.86, pp.375-388.